

Contribution from the Department of Chemistry, University of York, York YO1 5DD, U.K., and Department of Physical Sciences, Oxford Polytechnic, Oxford OX3 0BP, U.K.

## Vibrational Spectra of Terminal Metal Hydrides: Solution and Matrix-Isolation Studies of $[(\eta\text{-C}_5\text{H}_5)_2\text{MH}_n]^{x+}$ (M = Re, Mo, W, Nb, Ta; $n = 1\text{-}3$ ; $x = 0, 1$ )

Reuben B. Girling,<sup>1a</sup> Peter Grebenik,<sup>1b</sup> and Robin N. Perutz\*<sup>1a</sup>

Received May 21, 1985

The solution Raman spectra of  $\text{Cp}_2\text{MoH}_2$ ,  $\text{Cp}_2\text{WH}_2$ ,  $\text{Cp}_2\text{ReH}$ ,  $[\text{Cp}_2\text{MoH}_3]^+$ ,  $[\text{Cp}_2\text{WH}_3]^+$ , and  $[\text{Cp}_2\text{ReH}_2]^+$  are reported in the MCp and MH stretching regions, together with IR data for the  $\nu(\text{MH})$  region (Cp =  $\eta\text{-C}_5\text{H}_5$ ). Polarization measurements allow the identification of the  $a_1$ ,  $\nu(\text{MCp}_2)$  and  $\nu(\text{MH}_n)$  modes. IR spectra are reported for the neutral complexes above, and their  $^2\text{H}$ -substituted analogues,  $\text{Cp}_2\text{MD}_n$  and  $(\eta\text{-C}_5\text{D}_5)_2\text{MH}_n$ , isolated in Ar, CO,  $\text{N}_2$ , and  $\text{CH}_4$  matrices. IR data for matrix-isolated  $\text{Cp}_2\text{MH}_3$  (M = Nb, Ta) and Raman data for  $\text{Cp}_2\text{WH}_2$  are also included. Most of the skeletal vibrations of  $\text{Cp}_2\text{MD}_n$  may be identified from these spectra. The results for  $\text{Cp}_2\text{ReH}$  and isotopomers are tested against a model in which the  $\text{C}_5\text{H}_5$  unit is approximated by a point mass. The large changes in  $\nu(\text{MH}_n)$  induced by variation of the metal and by protonation are discussed. The exceptional width of  $\nu(\text{MH}_n)$  bands and their susceptibility to matrix-induced splitting are associated with the conformation of the  $\text{C}_5\text{H}_5$  rings.

### Introduction

The pivotal role of metal-hydrogen covalent bonds in organometallic and coordination chemistry has stimulated numerous studies of the nature of these bonds by diffraction, photoelectron spectroscopy, and photochemical, thermochemical, and other methods.<sup>2-8</sup> However, the use of IR spectroscopy has usually been confined to a diagnostic role. Recently, it has been recognized that a more detailed knowledge of IR spectra, particularly of cluster hydrides, can facilitate assignment of IR and EELS spectra of adsorbed molecules.<sup>9,10</sup> The majority of reports of IR spectra of terminal metal hydrides have identified M-H stretching modes only, but exceptions include the recently characterized matrix species  $\text{FeH}_2$  and  $\text{MnH}_2$ <sup>11,12</sup> and the rhenium polyhydrides.<sup>13</sup> The deformation modes of  $\text{ReH}_9^{2-}$ ,  $\text{ReH}_8(\text{PR}_3)^-$ , and  $\text{ReH}_7(\text{PR}_3)_2$  were identified in the 695-820- $\text{cm}^{-1}$  region.

In this paper we report on (i) IR spectra and Raman spectra of bis( $\eta$ -cyclopentadienyl)metal hydrides and isoelectronic cations in solution and (ii) IR spectra of the neutral hydrides and their  $^2\text{H}$ -substituted derivatives isolated under high dilution in argon, carbon monoxide, nitrogen, and methane matrices at 12-20 K. These studies avoid the solid state, which has represented a significant limitation to most previous vibrational data on hydrides.<sup>14,15</sup> By using Raman polarization data and isotopic substitution, we are able to identify many more modes than hitherto. We discuss the spectra of  $\text{MCp}_2\text{H}_n$  complexes in terms of  $\text{MX}_2\text{H}_n$  models, where the cyclopentadienyl ring (Cp =  $\eta\text{-C}_5\text{H}_5$ ) is represented by the point mass X. This paper represents a sequel to our papers on the photochemistry of  $\text{Cp}_2\text{MH}_n$ , in which some IR spectra of these complexes are illustrated.<sup>16,17</sup>

### Experimental Section

The experimental arrangement for matrix isolation and IR spectroscopy has been described in our papers on the photochemistry of  $\text{Cp}_2\text{MH}_n$  complexes.<sup>16,17</sup> The syntheses of these complexes together with most of the isotopically substituted derivatives are described in the same papers or in their references.

The isotopic derivative  $\text{Cp}_2\text{WHD}$  was synthesized by reaction of a toluene suspension of  $[\text{Cp}_2\text{W}(\text{H})\text{Li}]_4$  with  $\text{CH}_3\text{OD}$  at  $-5^\circ\text{C}$ .<sup>18</sup> The proportion of  $\text{Cp}_2\text{WHD}$  was estimated by NMR integration after a single pulse. For instance, a sample containing 70%  $\text{Cp}_2\text{WHD}$  and 30%  $\text{Cp}_2\text{WH}_2$  was obtained from an initial sample of 0.25 mmol of  $\text{Cp}_2\text{WH}_2$ .

A 400-MHz  $^1\text{H}$  spectrum ( $\text{C}_6\text{D}_6$  solution) of this sample with the cyclopentadienyl protons decoupled showed hydridic protons as follows:  $\text{Cp}_2\text{WH}_2$ ,  $\delta = -12.55$  (s,  $J_{\text{WH}} = 72.8$  Hz);  $\text{Cp}_2\text{WHD}$ ,  $\delta = -12.54$  (t,  $J_{\text{HD}} = 1.4$  Hz,  $J_{\text{WH}} = 72.9$  Hz). This indicates a downfield shift on deuteration of 0.01 ppm. A peak 0.005 ppm upfield of  $\text{Cp}_2\text{WH}_2$  with the same  $J_{\text{WH}}$  may be associated with a small proportion of the ring-deuterated material  $(\eta\text{-C}_5\text{H}_5)(\eta\text{-C}_5\text{H}_4\text{D})\text{WH}_2$ . The relative intensities of  $\nu(\text{MH})$  and  $\nu(\text{MD})$  in the matrix IR spectra were consistent with the NMR measurements, if the intrinsic intensity per hydride or deuteride is constant. This relation was also assumed for other deuterated samples. The intensities of the 906- $\text{cm}^{-1}$  ( $\text{Cp}_2\text{WH}_2$ ) and 884- $\text{cm}^{-1}$  ( $\text{Cp}_2\text{WHD}$ )

Table I. Skeletal Modes of  $\text{Cp}_2\text{MH}_n$  under  $\text{C}_{2v}$  Symmetry

	$\text{Cp}_2\text{MH}$	$\text{Cp}_2\text{MH}_2$	$\text{Cp}_2\text{MH}_3$
$\nu(\text{MH}_n)$	$a_1$	$a_1 + b_1$	$2a_1 + b_1$
$\nu(\text{MCp}_2)$	$a_1 + b_2$	$a_1 + b_2$	$a_1 + b_2$
$\delta(\text{MH}_n)$	$b_1 + b_2$	$a_1 + (a_2) + b_1 + b_2$	$a_1 + (a_2) + 2b_1 + 2b_2$
$\delta(\text{MCp}_2)$	$a_1$	$a_1$	$a_1$

bands were also approximately consistent with the NMR measurements. The 872- $\text{cm}^{-1}$  band (intense in  $\text{Cp}_2\text{WD}_2$ ) was far weaker, setting an upper limit of ca. 12% to the  $\text{Cp}_2\text{WD}_2$  content (see Figure 1).

The Raman spectrum of matrix-isolated  $\text{Cp}_2\text{WH}_2$  was measured on a Spex Ramalog 4 instrument and excited by 100 mW of 514.5-nm radiation from a Spectra-Physics Ar<sup>+</sup> laser. The Raman spectra of solutions under an argon atmosphere were measured on a Jobin-Yvon Ramanor HG2 spectrometer using a spinning cell and excited by 0.3-2.5 W of 647.1-nm radiation from a Spectra-Physics 170 Kr<sup>+</sup> laser. Several spectra were accumulated via a Nicolet computer in each run. The spectrometer is described in more detail elsewhere.<sup>19</sup> In both solution and matrix Raman experiments, slit widths of 5  $\text{cm}^{-1}$  were employed and spectra were calibrated with the Ne atomic lines. Wavenumbers should be accurate to  $\pm 3$   $\text{cm}^{-1}$  for sharp bands and  $\pm 4$   $\text{cm}^{-1}$  for broader bands.

- (1) (a) University of York. (b) Oxford Polytechnic.
- (2) Moore, D. S.; Robinson, S. D. *Chem. Soc. Rev.* **1983**, *12*, 415. Roundhill, D. M. *Adv. Organomet. Chem.* **1975**, *13*, 273.
- (3) Kaesz, H. D.; Saillant, R. B. *Chem. Rev.* **1972**, *72*, 231.
- (4) Green, M. L. H.; Jones, D. J. *Adv. Inorg. Chem. Radiochem.* **1965**, *7*, 115.
- (5) Bau, R.; Teller, R. G.; Kirtley, S. W.; Koetzle, T. F. *Acc. Chem. Res.* **1979**, *12*, 175. Teller, R. G.; Bau, R. *Struct. Bonding (Berlin)* **1981**, *44*, 1.
- (6) Cowley, A. H. *Prog. Inorg. Chem.* **1979**, *26*, 45.
- (7) Green, J. C. *Struct. Bonding (Berlin)* **1981**, *43*, 37.
- (8) (a) Pearson, R. G. *Chem. Rev.* **1985**, *85*, 41. (b) Calado, J. C.; Dias, A. R.; Martinho-Simoes, J. A.; Ribiero da Silva, M. A. V. *J. Organomet. Chem.* **1979**, *174*, 77.
- (9) Andrews, L. A.; Jayasooriya, U. A.; Powell, D. B.; Sheppard, N.; Jackson, P. F.; Johnson, B. F. G.; Lewis, J. *Inorg. Chem.* **1980**, *19*, 3033.
- (10) Howard, M. W.; Jayasooriya, U. A.; Kettle, S. F. A.; Powell, D. B.; Sheppard, N. *J. Chem. Soc., Chem. Commun.* **1979**, 18.
- (11) Ozin, G. A.; McCaffrey, J. G. *J. Am. Chem. Soc.* **1984**, *106*, 807.
- (12) Ozin, G. A.; McCaffrey, J. G. *J. Phys. Chem.* **1984**, *88*, 645.
- (13) Ginsberg, A. P.; Miller, J. M.; Koubek, E. *J. Am. Chem. Soc.* **1961**, *83*, 4909. Ginsberg, A. P. *Chem. Commun.* **1968**, 857. Chatt, J.; Coffey, R. S. *J. Chem. Soc. A* **1969**, 1963.
- (14) Fritz, H. P. *Adv. Organomet. Chem.* **1964**, *1*, 239.
- (15) Adams, D. M. "Metal-Ligand and Related Vibrations"; Arnold: London, 1967.
- (16) (a) Chetwynd-Talbot, J.; Grebenik, P.; Perutz, R. N.; Powell, M. H. A. *Inorg. Chem.* **1983**, *21*, 1675. (b) Baynham, R. F. G.; Chetwynd-Talbot, J.; Grebenik, P.; Perutz, R. N.; Powell, M. H. A. *J. Organomet. Chem.* **1985**, *284*, 229.
- (17) (a) Chetwynd-Talbot, J.; Grebenik, P.; Perutz, R. N. *Inorg. Chem.* **1982**, *21*, 3647. (b) Cox, P. A.; Grebenik, P.; Robinson, M. D.; Grinter, R.; Stern, D. R. *Inorg. Chem.* **1983**, *22*, 3614.
- (18) Francis, B. R.; Green, M. L. H.; Luong-thi, T.; Moser, G. A. *J. Chem. Soc., Dalton Trans.* **1976**, 1339.
- (19) Ernstbrunner, E.; Girling, R. B.; Grossman, W. E. L.; Hester, R. E. *J. Chem. Soc., Perkin Trans. 2* **1977**, 177.

\* To whom correspondence should be addressed; no reprints available.

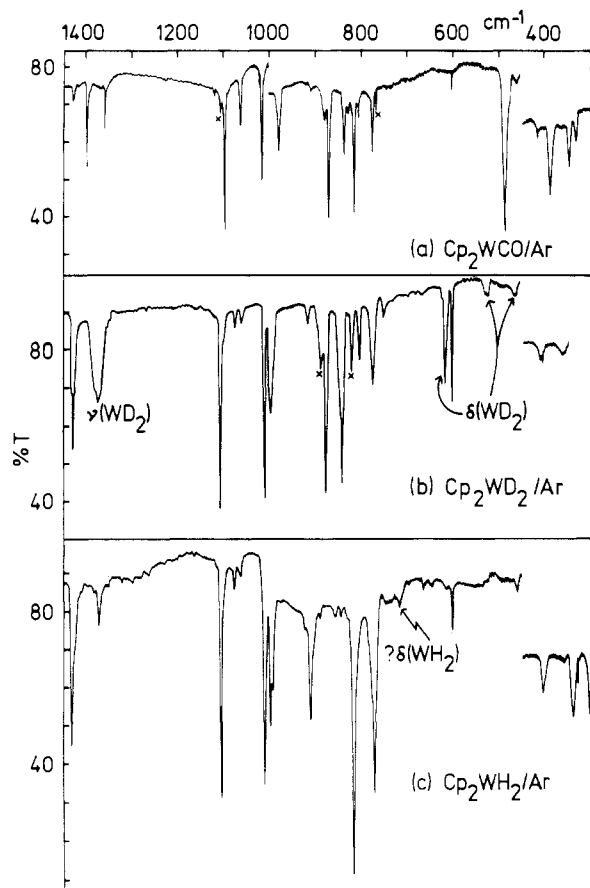


**Figure 1.** Argon matrix IR spectra at 12 K: (a)  $\text{Cp}_2\text{WCO}$  ( $X = \text{Cp}_2\text{WH}_2$  impurity, deposition time  $t_d = 210$  min, sample sublimation temperature  $T_s = 315$  K, 1.5 mmol of Ar); (b)  $\text{Cp}_2\text{WD}_2/\text{Cp}_2\text{WHD}$  ( $X = \text{Cp}_2\text{WHD}$ ,  $[\text{W}]\text{D}_2/[\text{W}]\text{HD} = 3.3$ ,  $t_d = 360$  min,  $T_s = 310\text{--}322$  K, 1.9 mmol of Ar); (c)  $\text{Cp}_2\text{WH}_2$  ( $t_d = 180$  min,  $T_s = 323$  K).

Corresponding IR measurements should have error bars of  $\pm 1$  and  $\pm 2$   $\text{cm}^{-1}$ .

IR spectra of solutions were measured in cells that had been purged with argon prior to filling. For aqueous solutions matched  $\text{CaF}_2$  cells of 0.05-mm pathlength were employed.

Force constant calculations<sup>20</sup> were performed by the GF matrix method with use of the program SOTONVIBP, which generates refined force constants and calculated frequencies from a trial set of atomic coordinates, masses, internal coordinates, and approximate force constants.

## Results

**I. Vibrations of  $\text{MH}_n$  and  $(\eta\text{-C}_5\text{H}_5)_2\text{M}$  Units.** The skeletal modes of  $\text{Cp}_2\text{MH}_n$  ( $n = 1\text{--}3$ ) are summarized in Table I. Recognition of  $\nu_{\text{MH}}$  stretching modes is usually straightforward, but identification of MH deformation modes is facilitated by first identifying the characteristic IR absorptions of the  $\text{Cp}_2\text{M}$  unit. The metal carbonyls  $\text{Cp}_2\text{MCO}$  ( $\text{M} = \text{Mo}, \text{W}$ ) can give us this information for the region  $1450\text{--}600$   $\text{cm}^{-1}$ , free of interference from the vibrations of other ligands (see Figure 1a of this paper and Table I of ref 16a). However, for the region  $450\text{--}250$   $\text{cm}^{-1}$  we must look to the hydrides (see below and Figure 1c). The observed spectra (with band positions in  $\text{cm}^{-1}$ ) are summarized in approximate form below, with assignments based on the analysis of parallel sandwich molecules:<sup>14,21</sup>

1420–1350	C–C str	3 bands
1110–1090	ring breathing	1 band
1060–980	parallel C–H def	3 bands
880–870	parallel C–C–C def	2 bands
835–770	perpendicular C–H def	4 bands
590–610	perpendicular C–C–C def	1 band
450–250	metal–ring str and tilt	3 bands

**Table II.** IR and Raman Spectra of  $\text{Cp}_2\text{MH}_n$  and  $[\text{Cp}_2\text{MH}_n]^+$  in Solution ( $\bar{\nu}/\text{cm}^{-1}$ )<sup>a</sup>

	Raman	IR
$\text{Cp}_2\text{ReH}$	2019 p, 391 dp, 344 p	2013
$\text{Cp}_2\text{WH}_2$	1898 p, 385 dp, 325 p	1890
$\text{Cp}_2\text{MoH}_2$	1833 p, 377 dp, 322 p	1823
$\text{Cp}_2\text{TaH}_3$	1756 p, 1785 p, sh, 352 dp, 294 p	
$[\text{Cp}_2\text{ReH}_2]^+$	2061 p, 397 dp, 352 p	
$[\text{Cp}_2\text{WH}_3]^+$	1955 p, 1998 p, sh, 385 dp, 336 p	~1945
$[\text{Cp}_2\text{MoH}_3]^+$	1910 p, 1932 p, 379 dp, 331 p	~1915

<sup>a</sup>The solvent is thf for neutral molecules and aqueous HCl for cations.

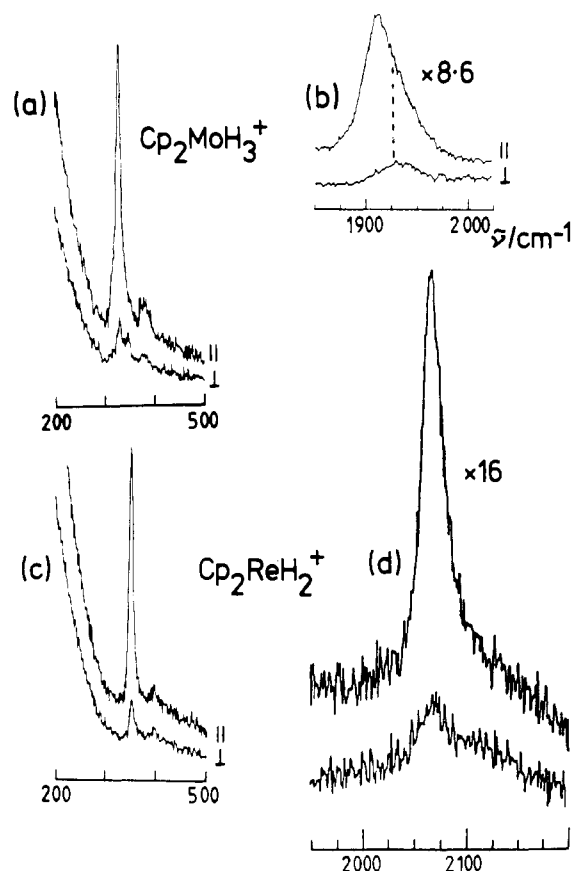


**Figure 2.** Raman spectra (647.1-nm excitation) measured at 300 K in a spinning cell of argon-saturated solutions: (a)  $[\text{Cp}_2\text{MoH}_3]^+$ ,  $\nu(\text{MoCp}_2)$  region (slits 1 mm, power 2.5 W, 1 scan with  $1\text{-cm}^{-1}$  steps); (b)  $[\text{Cp}_2\text{MoH}_3]^+$ ,  $\nu(\text{MoH}_3)$  region (conditions as for (a) but 32 scans accumulated and ordinate expansion  $\times 8.6$ ; notice noncoincidence of parallel and perpendicularly polarized maxima); (c)  $[\text{Cp}_2\text{ReH}_2]^+$ ,  $\nu(\text{ReCp}_2)$  region (slits 0.8 mm, power 2 W, 4 scans with  $1\text{-cm}^{-1}$  steps); (d)  $[\text{Cp}_2\text{ReH}_2]^+$ ,  $\nu(\text{ReH}_2)$  region (conditions as for (c) but 16 scans accumulated and ordinate expansion  $\times 16$ ). In each case, spectra are shown with the analyzer parallel (above) and perpendicular (below) to the laser polarization.

Invariably there is an excess of predicted bands over observed. For instance, we expect six modes in the low-frequency region: ring–metal–ring stretch ( $a_1 + b_2$ ) and ring tilt ( $a_1 + a_2 + b_1 + b_2$ ). Only the  $a_2$  mode is IR inactive, yet three bands rather than the expected five are observed. However, it is hardly surprising that modes such as  $\nu_{\text{sym}}(\text{MCp}_2)$  should be very weak since the ring–metal–ring angle lies in the  $140\text{--}155^\circ$  range. The corresponding bands of the metallocenes are very prominent in their Raman spectra,<sup>21</sup> and we have found similar intense bands in the spectra of  $\text{Cp}_2\text{MH}_n$ .

**II. Raman and IR Spectra in Solution.** The Raman spectra of the neutral complexes  $\text{Cp}_2\text{ReH}$ ,  $\text{Cp}_2\text{WH}_2$ , and  $\text{Cp}_2\text{MoH}_2$  measured in tetrahydrofuran solution (thf) each exhibit a very

(20) Beattie, I. R.; Cheetham, N.; Gardiner, M.; Rogers, D. E.; *J. Chem. Soc. A* **1971**, 2240.

(21) Aleksanyan, V. T. *Vib. Spectra Struct.* **1982**, *11*, 107.

Table IV. Observed and Calculated Skeletal Vibrations of Cp<sub>2</sub>ReH and Isotopic Derivatives in a CO Matrix ( $\bar{\nu}/\text{cm}^{-1}$ )<sup>a</sup>

		Cp <sub>2</sub> ReH		Cp <sub>2</sub> ReD			$(\eta^5\text{-C}_5\text{D}_5)_2\text{ReH}$		
		obsd	calcd	obsd	calcd	error	obsd	calcd	error
$\nu(\text{ReH})$	a <sub>1</sub>	2032	2032.0	1448	1441.2	-6.8	...	...	...
$\nu(\text{ReX}_2)$	a <sub>1</sub>	348	348.0	...	347.9	...	...	335.8	...
$\delta(\text{ReX}_2)$	a <sub>1</sub>	...	81.5	...	81.4	...	...	79.6	...
$\delta_{\text{oop}}(\text{ReH})$	b <sub>1</sub>	846	846.0	640	649.6	9.6	835	843.5	8.5
$\delta_{\text{ip}}(\text{ReH})$	b <sub>2</sub>	515	515.0	457	377.2	-79.8	502	514.6	12.6
$\nu_a(\text{ReX}_2)$	b <sub>2</sub>	358	358.0	356	347.5	-8.5	342	350.3	8.3

force constants (N m<sup>-1</sup>):  $f_t(\text{ReH}) = 243.7$ ,  $f_r(\text{ReX}) = 375.0$ ,  $f_{rr}(\text{ReH}/\text{ReX}) = 2.0$ ,  $f_{rr}(\text{ReX}/\text{ReX}') = 69.7$ ,  $f_\delta(\text{HReX}) = 47.2$ ,  $f_\delta(\text{XReX}) = 7.8$ ,  $f_{\delta\delta}(\text{HReX}/\text{HReX}') = 25.6$ ,  $f_{\delta\delta}(\text{HReX}/\text{XReX}') = 6.5$ ,  $f_\delta(\text{ReH}_{\text{oop}}) = 97.3$ ,  $f_\delta(\text{ReX}/\text{HReX}) = 12.8$

<sup>a</sup> ip and oop indicate in and out of the ReX<sub>2</sub>H plane. X =  $\eta^5\text{-C}_5\text{H}_5$ .

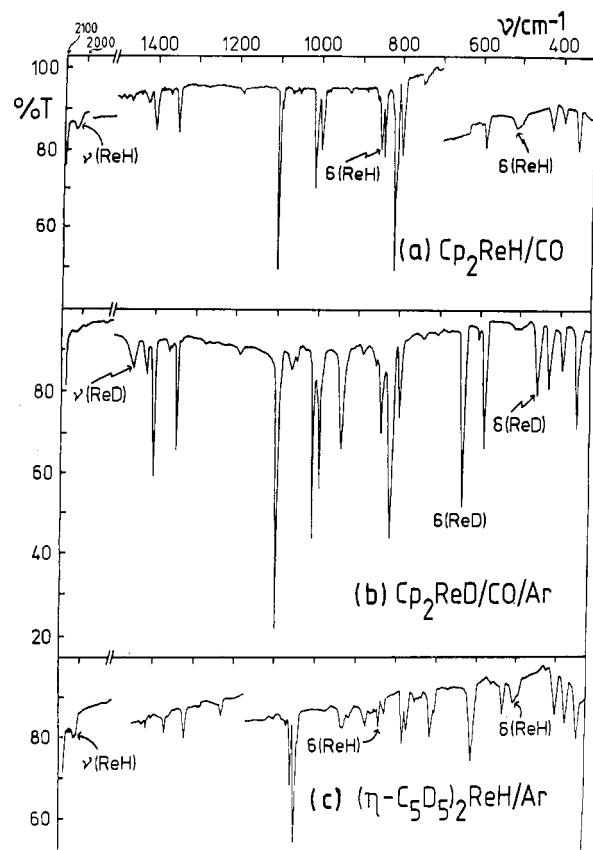


Figure 3. IR spectra at 16–19 K showing ReH(D) stretching and deformation vibrations and effect of ring deuteration on Cp<sub>2</sub>ReH: (a) Cp<sub>2</sub>ReH in CO matrix ( $t_d = 240$  min,  $T_s = 320$  K); (b) Cp<sub>2</sub>ReD/Cp<sub>2</sub>ReH in CO/Ar matrix ( $[\text{ReD}]/[\text{ReH}] \approx 6$ , CO/Ar = 1.0,  $t_d = 180$  min,  $T_s = 333$  K, 2.2 mmol of CO/Ar); (c)  $(\eta^5\text{-C}_5\text{D}_5)_2\text{ReH}$  in CO matrix ( $t_d = 130$  min,  $T_s = 316$  K, 3.9 mmol of CO).

intense polarized band between 320 and 350 cm<sup>-1</sup>, which we assign to  $\nu_{\text{sym}}(\text{CpMCP})$ , and a weaker polarized band in the MH stretching region,  $\nu(\text{MH}_n)$  (Table II, Figure 2). The corresponding IR bands in the MH stretching region are located 6–10 cm<sup>-1</sup> to lower frequency than the Raman bands. The full width at half-maximum (fwhm) of the bands is 40–45 cm<sup>-1</sup> in both IR and Raman spectra. The discrepancy between IR and Raman spectra of Cp<sub>2</sub>ReH lies outside our calibration errors. We believe that it is a genuine shift, which we ascribe to differences in the effect of inhomogeneous broadening (see Discussion). Because of this effect we are unable to establish from solution evidence alone whether the maxima in the IR spectra of Cp<sub>2</sub>MH<sub>2</sub> should be assigned to symmetric or antisymmetric vibrations. However, we note that the crystallographic H–M–H angle (75.5° for Cp<sub>2</sub>MoH<sub>2</sub>)<sup>22</sup> leads to a predicted intensity ratio  $I_{\text{sym}}/I_{\text{asym}} = 1.7$  if we assume harmonicity and energy factoring of  $\nu(\text{MH})$  vibrations.<sup>23</sup> On this basis we prefer to assign the IR maxima to  $\nu_{\text{sym}}(\text{MH}_2)$ .

(22) Schultz, A. J.; Stearley, K. L.; Williams, J. M.; Mink, R.; Stucky, G. D. *Inorg. Chem.* **1977**, *16*, 3303.

(23) See e.g.: Haines, L. M.; Stiddard, M. B. H. *Adv. Inorg. Chem. Radiochem.* **1969**, *12*, 53.

The Raman spectra of [Cp<sub>2</sub>ReH<sub>2</sub>]<sup>+</sup>, [Cp<sub>2</sub>WH<sub>3</sub>]<sup>+</sup>, and [Cp<sub>2</sub>MoH<sub>3</sub>]<sup>+</sup>, recorded in ca. 0.2 M HCl, show a pattern similar to that of the neutral molecules with intense polarized metal–ring modes and weaker MH modes. The Raman spectra of the trihydride cations show two polarized  $\nu(\text{MH}_3)$  bands in accordance with expectations (Tables I and II), but their IR counterparts show very weak, broad bands with ill-defined maxima even when recorded at higher concentration in ca. 0.5 M HCl (see Note Added in Proof).

### III. Matrix IR Spectra of Cp<sub>2</sub>ReH, Cp<sub>2</sub>ReD, and $(\eta^5\text{-C}_5\text{D}_5)_2\text{ReH}$ .

The matrix IR spectra of the above isotopomers are illustrated in Figure 3 and listed in Table III (supplementary material). The band at ca. 2030 cm<sup>-1</sup> is easily identified as  $\nu(\text{ReH})$ . The bands of Cp<sub>2</sub>ReH in the 950–1450-cm<sup>-1</sup> region together with the very intense mode at 812 cm<sup>-1</sup> can be identified as vibrations of the Cp<sub>2</sub>Re moiety as can the three bands below 450 cm<sup>-1</sup> (see section I above). Furthermore, by comparison with the spectrum of Cp<sub>2</sub>ReD we identify bands at 846 and 515 cm<sup>-1</sup> (CO matrix, Figure 3) as ReH deformation modes. Deuteration at the hydridic position shifted these bands considerably and resulted in the appearance of a prominent band at 936 cm<sup>-1</sup>, apparently at the expense of the weak 928-cm<sup>-1</sup> band of Cp<sub>2</sub>ReH. The remaining bands of Cp<sub>2</sub>ReH were shifted by less than 4 cm<sup>-1</sup>. We have found that M–H stretching modes are characteristically broad in matrices and in solution (see above). The pair of bands at 515 (Cp<sub>2</sub>ReH) and 457 (Cp<sub>2</sub>ReD) cm<sup>-1</sup> is also unusually broad.

If the point-mass description of the rings is a useful approximation, we should find that use of  $(\eta^5\text{-C}_5\text{D}_5)_2\text{ReH}$  causes the retention of the Re–H modes while most of the remaining modes are shifted. Indeed we find bands for the Re–H modes of  $(\eta^5\text{-C}_5\text{D}_5)_2\text{ReH}$  shifted by factors of 1.001, 1.013, and 1.066 (Tables III and IV). In contrast, the C–H deformations in the region 760–1060 cm<sup>-1</sup> are shifted by factors of 1.30–1.344. We note that the shifts in the C–C–C modes, in the ring breathing modes, and in the Re–ring vibrations are considerably smaller, varying from 1.021 to 1.116. Thus this analysis also confirms the basic assignments for the Cp<sub>2</sub>M unit given in the preceding section.

We have used both valence force-field and product rule calculations to test the point-mass approximation and to help assign the spectra. The calculations assumed Re–H and Re–X distances of 1.67 and 1.99 Å and an X–Re–X angle of 153.3° as in the recent structure of K[18-crown-6]Cp<sub>2</sub>MoH.<sup>24</sup> The most satisfactory assignment according to both methods is that shown in Table IV, which also summarizes the force constant calculations. Notice that these calculations were designed to give an exact fit to the Cp<sub>2</sub>ReH frequencies rather than a least-squares fit to all the frequencies. The errors to the point-mass approximation turn out to be very substantial, reaching 80 cm<sup>-1</sup> for Cp<sub>2</sub>ReD and 13 cm<sup>-1</sup> for  $(\eta^5\text{-C}_5\text{D}_5)_2\text{ReH}$ . As anticipated, the largest errors arise in the deformations of Cp<sub>2</sub>ReD, since the model fails to take account of coupling to other modes of the rings. Thus the ReH deformation in the ReX<sub>2</sub>H plane is shifted by only 50% of the calculated value on deuteration. The largest error may be reduced to 62 cm<sup>-1</sup> by placing  $\nu_a(\text{ReX}_2)$  at 395 cm<sup>-1</sup>, although we prefer the assignment  $\nu_a(\text{ReX}_2) = 358$  cm<sup>-1</sup> on comparison with  $\nu_s(\text{ReX}_2)$ .

### IV. Matrix IR and Raman Spectra of Cp<sub>2</sub>MH<sub>2</sub>, Cp<sub>2</sub>MD<sub>2</sub>, $(\eta^5\text{-C}_5\text{D}_5)_2\text{MH}_2$ , and $(\eta^5\text{-C}_5\text{D}_5)_2\text{MD}_2$ (M = Mo, W). a. M–H and

(24) Bandy, J. A.; Berry, A.; Green, M. L. H.; Perutz, R. N.; Prout, K.; Verpauw, J. N. *J. Chem. Soc., Chem. Commun.* **1984**, 729.

**Table V.** Skeletal Vibrations of  $\text{Cp}_2\text{MH}_2$  ( $\text{M} = \text{Mo}, \text{W}$ ) and Isotopic Derivatives: Infrared Data for Argon Matrices ( $\nu/\text{cm}^{-1}$ )

	$\text{Cp}_2\text{MoH}_2$	$\text{Cp}_2\text{MoD}_2$	$(\eta\text{-C}_5\text{D}_5)_2\text{-MoH}_2$	$\text{Cp}_2\text{WH}_2$	$\text{Cp}_2\text{WHD}$	$\text{Cp}_2\text{WD}_2$	$(\eta\text{-C}_5\text{D}_5)_2\text{-WH}_2$	$(\eta\text{-C}_5\text{D}_5)_2\text{-WD}_2$
$\nu_{\text{sym}}(\text{MH}_2)$	1832	1317	1833	1908/1904	1914/1903	1375/1365	1900	1367
$\nu_{\text{asym}}(\text{MH}_2)$					1374/1366			
$\delta_{\text{sym}}(\text{MH}_2)$		607			617	614		624
$\rho(\text{MH}_2)$	670	505	666	730	589	524	737	520
$\delta_{\text{asym}}(\text{MH}_2)$	540	474	547			463		446
$\nu_{\text{sym}}(\text{MX}_2)$				330 <sup>a</sup>				
$\nu_{\text{asym}}(\text{MX}_2)$	321	318	304	339	338	ca. 339	323	320
$\delta(\text{MX}_2)$				153 <sup>a</sup>				

<sup>a</sup>  $\text{CH}_4$  matrix (Raman data).

**M–D Stretching Region.** The Raman spectrum of  $\text{Cp}_2\text{WH}_2$  in a  $\text{CH}_4$  matrix shows a broad  $\nu(\text{W–H})$  band at  $1907\text{ cm}^{-1}$  with a shoulder at  $1900\text{ cm}^{-1}$ . The corresponding IR spectrum of  $\text{Cp}_2\text{WH}_2$  isolated in  $\text{CH}_4$  at ca. 3 times higher dilution shows bands at  $1904$  and  $1898$  ( $\text{sh}$ )  $\text{cm}^{-1}$  (Figure 4ab). The bands are still extremely broad:  $\text{fwhm}(\text{Raman}) = 27$ ,  $\text{fwhm}(\text{IR}) = 23\text{ cm}^{-1}$ . Considering the strong polarization of this band in the solution Raman measurements, both IR and Raman bands must be assigned to  $\nu_{\text{sym}}(\text{WH}_2)$ . The shoulder cannot be associated with  $\nu_{\text{asym}}(\text{WH}_2)$ .

The spectrum of  $\text{Cp}_2\text{WH}_2$  in the  $\nu(\text{WH}_2)$  region is at its sharpest when isolated at high dilution in argon (Figure 4c). The fwhm value is reduced to ca.  $6\text{ cm}^{-1}$ ; however, this is still broad by matrix standards and broader than most other bands in the spectrum. There are several possible contributors to the presence of six bands spread over  $50\text{ cm}^{-1}$  in this spectrum: two fundamentals, coincident overtone and combination bands, multiple conformations, multiple sites in the matrix. The corresponding vibrations of  $\text{Cp}_2\text{MD}_2$  are observed between  $1300$  and  $1400\text{ cm}^{-1}$  and also show several components. More evidence for the origin of the splittings comes from the spectrum of  $\text{Cp}_2\text{MHD}$ , since this molecule can have only one  $\nu(\text{M–H})$  fundamental and any resonance between  $\delta(\text{MH}_2)$  and  $\nu(\text{MH}_2)$  in the unsubstituted molecule would be disrupted in  $\text{Cp}_2\text{MHD}$  (compare the situation in hydrocarbons).<sup>25</sup> Thus we should expect only one band in the  $\nu(\text{MH})$  region for  $\text{Cp}_2\text{MHD}$ , unless multiple conformations or sites contribute.

The spectrum of a sample consisting of 70%  $\text{Cp}_2\text{WHD}$  and 30%  $\text{Cp}_2\text{WH}_2$  isolated in an argon matrix (see Experimental Section) showed broad structured bands for both  $\nu(\text{MH})$  and  $\nu(\text{WD})$  (Figure 4d). Similar conclusions are drawn from a matrix spectrum of a scrambled mixture containing  $\text{Cp}_2\text{MoD}_2$ ,  $\text{Cp}_2\text{MoHD}$ , and  $\text{Cp}_2\text{MoH}_2$  in proportions ca. 16:8:1. Finally, we note that the removal of coincidences between overtones/combinations of ring modes and  $\nu(\text{MoH})$  fails to simplify the spectrum: the IR spectrum of  $(\eta\text{-C}_5\text{D}_5)_2\text{MoH}_2$  again shows a set of components similar to that of  $\text{Cp}_2\text{MoH}_2$  (Figure 4e). We are driven to conclude that the splittings are caused by either multiple conformations or multiple sites in the matrix.

The influence of site effects can usually be modified by changing the matrix, yet we still observe several components of  $\nu(\text{MH})$  for  $\text{Cp}_2\text{WH}_2$  in  $\text{N}_2$ ,  $\text{CO}$ , and  $\text{CH}_4$  although the wavenumber spread is reduced relative to that in an argon matrix. Moreover, the shifts in the frequency of the most intense component are less than  $5\text{ cm}^{-1}$ . Thus this evidence points to a conformational origin of the splittings (see Discussion).

**b. M–H and M–D Deformation Region.** The IR spectra of  $\text{Cp}_2\text{MH}_2$  complexes in the region below  $1500\text{ cm}^{-1}$  are typically much sharper than those in the MH stretching region, with fwhm values of ca.  $2\text{ cm}^{-1}$ . Matrix splittings/conformational effects cause only minor perturbations, giving no more than two components separated by  $2\text{--}3\text{ cm}^{-1}$  at the highest dilution. Complete listings of wavenumbers are given in Table III.

At the outset of this paper we identified the pattern of vibrations for bent  $\text{MCp}_2$  fragments in the  $600\text{--}1400\text{-cm}^{-1}$  region by reference to  $\text{Cp}_2\text{MCO}$ . When we compare the spectra of  $\text{Cp}_2\text{MD}_2$

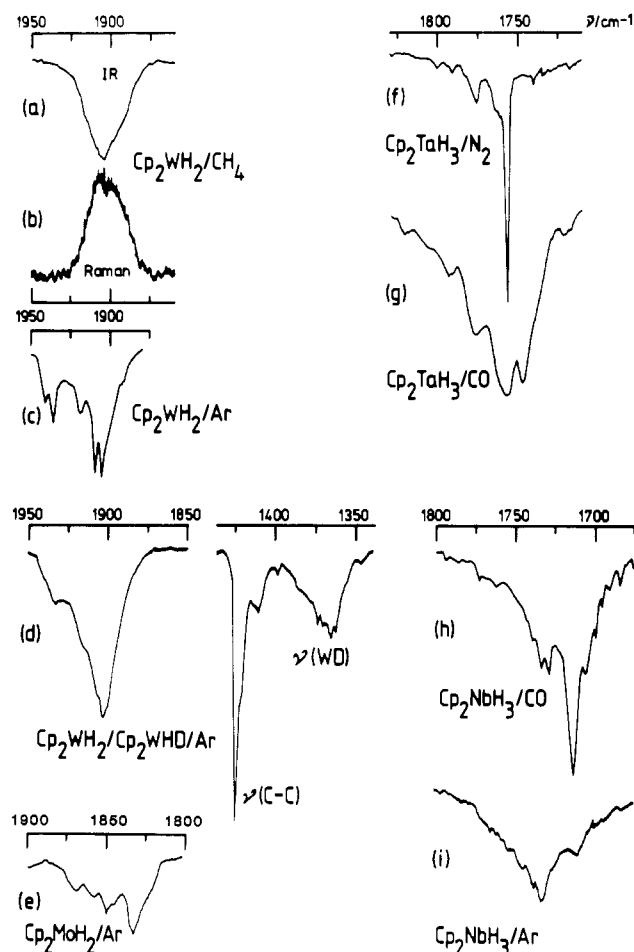


**Figure 4.** Matrix spectra in  $\nu(\text{MH}_n)$  and  $\nu(\text{MD}_n)$  regions: (a)  $\text{Cp}_2\text{WH}_2$  in  $\text{CH}_4$ ; (b)  $\text{Cp}_2\text{WH}_2$  in  $\text{CH}_4$  at 12 K (Raman,  $514.5\text{-nm}$  excitation, power  $100\text{ mW}$ , speed  $0.5\text{ cm}^{-1}\text{ s}^{-1}$ , period  $5\text{ s}$ , photon counter  $10^3$ ; note coincidence with IR spectrum); (c)  $\text{Cp}_2\text{WH}_2$  in Ar at extremely high dilution; (d)  $\text{Cp}_2\text{WH}_2/\text{Cp}_2\text{WHD}$  (1:2.5) in Ar, note width of  $\nu(\text{WH})$  and  $\nu(\text{WD})$  compared to that of  $\nu(\text{CC})$ ; (e)  $\text{Cp}_2\text{MoH}_2$  in Ar at very high dilution; (f)  $\text{Cp}_2\text{TaH}_3$  in  $\text{N}_2$  at extremely high dilution; (g)  $\text{Cp}_2\text{TaH}_3$  in  $\text{CO}$ ; (h)  $\text{Cp}_2\text{NbH}_3$  in  $\text{CO}$ ; (i)  $\text{Cp}_2\text{NbH}_3$  in Ar. All spectra are in IR absorption except (b) and were measured at  $16\text{--}19\text{ K}$ .

( $\text{M} = \text{Mo}, \text{W}$ ) to those of  $\text{Cp}_2\text{MCO}$ , we find patterns that compare favorably in frequency, intensity, and number of bands. In consequence, we are able to assign three M–D deformation modes to bands in the  $450\text{--}620\text{-cm}^{-1}$  region (Table V, Figures 1 and 5). These features are broader than the  $\text{C}_5\text{H}_5$  vibrations with fwhm values of ca.  $6\text{ cm}^{-1}$ . It proves to be much harder to pick out the  $\text{MH}_2$  deformations of  $\text{Cp}_2\text{MH}_2$  because the  $700\text{--}900\text{-cm}^{-1}$  region is perturbed so much that it bears little resemblance to  $\text{Cp}_2\text{MD}_2$  or  $\text{Cp}_2\text{MCO}$  (Figures 1 and 5). It seems likely that there is considerable mixing between the highest frequency  $\text{MH}_2$  deformation and the CH deformations. For this reason, some of the assignments in Table V are incomplete or tentative.

The assignments can be tested further by comparisons with  $(\eta\text{-C}_5\text{D}_5)_2\text{MH}_2$  ( $\text{M} = \text{Mo}, \text{W}$ ). All the intense bands of  $\text{Cp}_2\text{MH}_2$

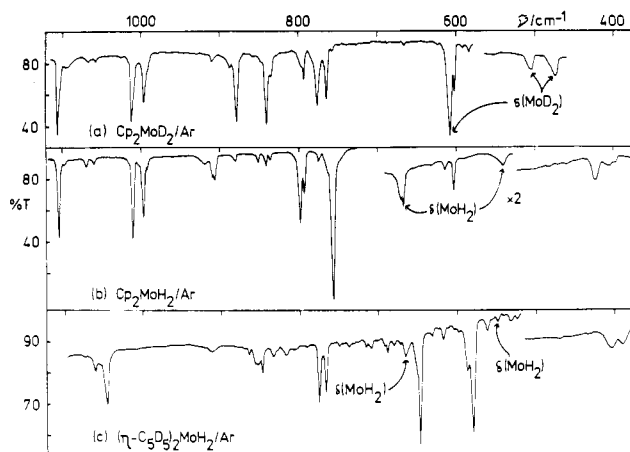


**Figure 5.** IR spectra below  $1150\text{ cm}^{-1}$  in Ar matrices at  $16\text{--}19\text{ K}$  showing  $\text{MoH}_2(\text{D}_2)$  deformation modes and effect of ring deuteration on  $\text{Cp}_2\text{MoH}_2$ : (a)  $\text{Cp}_2\text{MoD}_2/\text{Cp}_2\text{MoHD}$  ( $3.3:1$ ,  $t_d = 105\text{ min}$ ,  $T_s = 328\text{ K}$ ,  $5.6\text{ mmol}$  of Ar); (b)  $\text{Cp}_2\text{MoH}_2$  ( $t_d = 270\text{ min}$ ,  $T_s = 312\text{ K}$ ,  $3.1\text{ mmol}$  of Ar); (c)  $(\eta\text{-C}_5\text{D}_5)_2\text{MoH}_2$  ( $t_d = 120\text{ min}$ ,  $T_s = 323\text{ K}$ ,  $3.8\text{ mmol}$  of Ar).

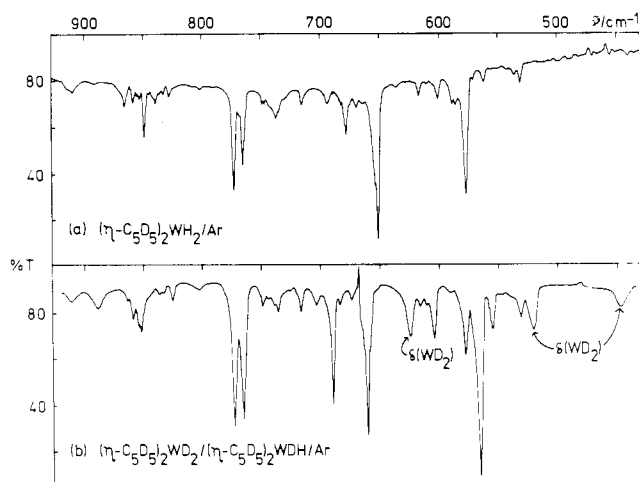


**Figure 6.** IR spectra below  $950\text{ cm}^{-1}$  in Ar matrices at  $16\text{--}19\text{ K}$  showing effect of ring deuteration and  $\text{WD}_2$  deformation modes on  $\text{Cp}_2\text{WH}_2$ : (a)  $(\eta\text{-C}_5\text{D}_5)_2\text{WH}_2$  ( $t_d = 150\text{ min}$ ,  $T_s = 333\text{ K}$ ,  $1.9\text{ mmol}$  of Ar); (b)  $(\eta\text{-C}_5\text{D}_5)_2\text{WD}_2/(\eta\text{-C}_5\text{D}_5)_2\text{WHD}$  ( $12:1$ ,  $t_d = 270\text{ min}$ ,  $T_s = 328\text{ K}$ ,  $3.1\text{ mmol}$  of Ar).

in the  $700\text{--}1150\text{-cm}^{-1}$  region shift by at least  $50\text{ cm}^{-1}$  on deuteration of the rings, and in many cases the shifts exceed  $200\text{ cm}^{-1}$ . In contrast, the bands assigned to  $\text{MH}_2$  deformation modes shift less than  $10\text{ cm}^{-1}$  (Figures 5 and 6). We have also obtained consistent data on  $(\eta\text{-C}_5\text{D}_5)_2\text{WD}_2$ . Again it is much more straightforward to assign the vibrations of  $[\text{W}]\text{D}_2$  than  $[\text{W}]\text{H}_2$  complexes (Figure 6).

The remaining skeletal vibrations are  $\nu_{\text{sym}}(\text{MX}_2)$ ,  $\nu_{\text{asym}}(\text{MX}_2)$ , and  $\delta(\text{MX}_2)$ . The polarization of the intense Raman band observed at ca.  $320\text{ cm}^{-1}$  in solution indicates an assignment to  $\nu_{\text{sym}}(\text{MX}_2)$ . This band has also been observed in the Raman spectrum of  $\text{Cp}_2\text{WH}_2$  in  $\text{CH}_4$ . Following this assignment, the IR band at ca.  $340\text{ cm}^{-1}$  should be assigned to  $\nu_{\text{asym}}(\text{MX}_2)$ . The Raman band at  $153\text{ cm}^{-1}$  is tentatively assigned to the  $\delta(\text{MX}_2)$  vibration. These assignments and the corresponding ones for the isotopically substituted derivatives and for  $\text{Cp}_2\text{MoH}_2$ , etc. are listed in Table V.

**V. Matrix IR Spectra of  $\text{Cp}_2\text{MH}_3$  ( $\text{M} = \text{Nb}, \text{Ta}$ ).** The trihydrides  $\text{Cp}_2\text{MH}_3$  ( $\text{M} = \text{Nb}, \text{Ta}$ ) have three fundamental M–H stretching vibrations (Table I). The Raman spectra of the iso-electronic cations  $[\text{Cp}_2\text{MH}_3]^+$  ( $\text{M} = \text{Mo}, \text{W}$ ) show two polarized components separated by  $22$  and  $43\text{ cm}^{-1}$ , respectively. The IR spectrum of  $\text{Cp}_2\text{TaH}_3$  isolated in a  $\text{N}_2$  matrix at very high dilution is sharp and shows three major components at  $1757$ ,  $1763$  (sh), and  $1777\text{ cm}^{-1}$ , which we tentatively associate with the fundamentals  $a_1$  (in phase),  $b_1$ , and  $a_1$  (out of phase) (Figure 4f). The

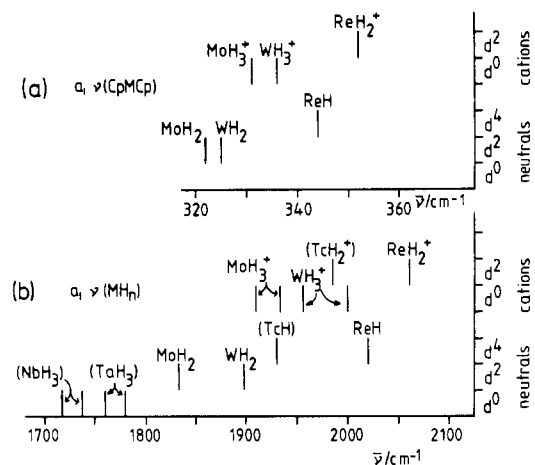


**Figure 7.** Schematic diagram of the trends in the solution Raman spectra of  $\text{Cp}_2\text{MH}_n$  and  $[\text{Cp}_2\text{MH}_{n+1}]^+$  according to d-electron count, showing (a) the polarized CpMCp vibration and (b) the polarized  $\text{MH}_n$  vibrations. The lines for  $\text{Cp}_2\text{NbH}_3$  and  $\text{Cp}_2\text{TaH}_3$  are based on matrix IR data. The lines for  $\text{Cp}_2\text{TcH}$  and  $[\text{Cp}_2\text{TcH}_2]^+$  are based on IR data (KBr disk) from: Fischer, E. O.; Schmidt, M. W. *Angew. Chem., Int. Ed. Engl.* **1967**, *6*, 93.

most intense component should be the in-phase  $a_1$  vibration. The corresponding spectra in CO and Ar matrices are complicated by broad bands and splitting into several components. The IR spectrum of  $\text{Cp}_2\text{NbH}_3$  in a CO matrix resembles that for  $\text{Cp}_2\text{TaH}_3$  in  $\text{N}_2$  although it is not so sharp. The most intense component is at  $1715\text{ cm}^{-1}$  with further bands at  $1707$ ,  $1730$ , and  $1735\text{ cm}^{-1}$  (Figure 4g–i).

#### Discussion

The observations described above pinpoint the totally symmetric  $\text{MH}_n$  vibrations for almost all members of the  $\text{Cp}_2\text{MH}_n$  series. Not only can we assign the IR  $\nu(\text{MH}_n)$  bands, but we are able to identify the M–D deformation modes of  $\text{Cp}_2\text{MD}_n$  and some deformation modes of  $\text{Cp}_2\text{MH}_n$ . The spectra of isotopically substituted  $\text{Cp}_2\text{ReH}$  derivatives suggest, via the force constant calculations, that there is significant mixing of the metal–hydrogen deformation modes but not of the stretching modes with ring modes. Such mixing is much more apparent in  $\text{Cp}_2\text{MH}_2$  than in  $\text{Cp}_2\text{MD}_2$ .

**Trends in  $\nu(\text{MH}_n)$ .** The striking variations in the  $a_1 \nu(\text{MH}_n)$  modes of the complexes are displayed in Figure 7. The frequencies change from  $1716\text{ cm}^{-1}$  for  $\text{Cp}_2\text{NbH}_3$  to  $2061\text{ cm}^{-1}$  for  $\text{Cp}_2\text{ReH}_2^+$ , equivalent to a 44% increase in M–H stretching force constant. Any mixing with ring modes is likely to be most effective for  $\text{Cp}_2\text{NbH}_3$ , implying that this estimate represents a lower limit. We have analyzed these changes in several ways, in each case using the average of the two  $a_1$  modes for  $[\text{Cp}_2\text{MH}_3]^{x+}$ : (i) As one moves from a  $4d$   $\text{Cp}_2\text{MH}_n$  complex to the corresponding  $5d$  complex,  $\nu(\text{MH}_n)$  increases by ca.  $60\text{ cm}^{-1}$ ; (ii) A similar increase is observed on protonation of  $\text{Cp}_2\text{MH}_n$  (representing a change from  $d^x$  to  $d^{x-2}$ ), but this average masks a range from  $42\text{ cm}^{-1}$  (Re) to  $88\text{ cm}^{-1}$  (Mo); (iii) the frequencies increase between adjacent isoelectronic cations (e.g.  $[\text{Cp}_2\text{WH}_3]^+ \rightarrow [\text{Cp}_2\text{ReH}_2]^+$ , representing a change from  $d^x$  to  $d^{x+2}$ ) by ca.  $74\text{ cm}^{-1}$  but by ca.  $120\text{ cm}^{-1}$  for adjacent isoelectronic neutral complexes. (iv) As one moves from a neutral complex to the isoelectronic cation (e.g.  $\text{Cp}_2\text{WH}_2 \rightarrow [\text{Cp}_2\text{ReH}_2]^+$ , no change in d-electron count) the frequency increases by ca.  $180\text{ cm}^{-1}$ , i.e. the sum of (ii) and (iii).

We may add to these observations our earlier finding that the values of  $\nu(\text{MH})$  for  $\text{Cp}_2\text{MH}$  ( $\text{M} = \text{Nb}, \text{Ta}$ ) are ca.  $25\text{ cm}^{-1}$  lower than the corresponding values for  $\text{Cp}_2\text{MH}_3$ . The values for  $\text{Cp}_2\text{M}(\text{H})\text{CO}$  lie between those for  $\text{Cp}_2\text{MH}_3$  and  $\text{Cp}_2\text{MH}$ .<sup>18</sup> These results lead to two further postulates based on the group V/VII comparison: (v) A change from  $\text{Cp}_2\text{MH}_3$  to  $\text{Cp}_2\text{MH}$  with no change of metal ( $d^0 \rightarrow d^2$ ) leads to a fall in  $\nu(\text{MH})$  of ca.  $25\text{ cm}^{-1}$ . (vi) A change from  $\text{Cp}_2\text{MH}$  to  $\text{Cp}_2\text{M}'\text{H}$  ( $d^2 \rightarrow d^4$ ) or from  $\text{Cp}_2\text{MH}(\text{L})$  to  $\text{Cp}_2\text{M}'\text{H}$  ( $d^2 \rightarrow d^4$ ) leads to an increase in  $\nu(\text{MH})$  of ca.  $290\text{ cm}^{-1}$ , representing an increase in force constant of ca.

36%. The trends for the neutral molecules may be summarized by the equation

$$\nu(\text{MH}_n) = 1688 + 55\delta + 136(x - 5) + 15(y - 3)$$

with an rms error of 5.1  $\text{cm}^{-1}$ , where  $\delta = 0$  for 4d metals and  $\delta = 1$  for 5d metals,  $x$  is the group of the periodic table to which the metal belongs, and  $y$  is its oxidation state. A modified equation may be applied to the complete set of neutral molecules and cations

$$\nu(\text{MH}_n) = 1686 + 59\delta + 131(x - 5) + 20(y - 3) + 24z$$

with an rms error of 13.2  $\text{cm}^{-1}$ , where  $z$  is the charge on the complex.

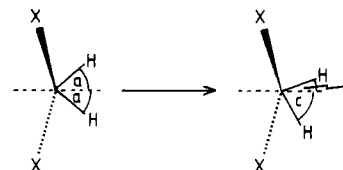
We conclude that M–H binding *improves substantially from 4d to 5d elements but even more markedly across a transition-metal period. The binding improves with increasing oxidation state*, but there is no competition for electron density between M–H bonds of an  $\text{MH}_n$  group. The lack of competition is in accord with the established presence of three orbitals which can bond in the  $\text{MH}_n$  plane.<sup>26</sup> Although such data have been available for individual compounds before,<sup>14</sup> such a large series of iso-electronic complexes helps to highlight and quantify the variations. Finally, we note that our data on  $\nu_{\text{sym}}(\text{CpMCp})$  support the existence of similar variations (as a percentage of the frequency) in MCp force constants.

Our conclusions are consistent with the sparse thermochemical data:  $\bar{D}(\text{M–H}) = 251$  ( $\text{Cp}_2\text{MoH}_2$ ) and 305  $\text{kJ mol}^{-1}$  ( $\text{Cp}_2\text{WH}_2$ ).<sup>8b</sup> Moreover, the order of thermal stability with respect to  $\text{H}_2$  loss runs  $\text{Cp}_2\text{NbH}_3 < \text{Cp}_2\text{TaH}_3 < \text{Cp}_2\text{MoH}_2$ . Thus  $\text{Cp}_2\text{NbH}_3$  and  $\text{Cp}_2\text{TaH}_3$  are thermal C–H activators at 80 and 100 °C, respectively, while  $\text{Cp}_2\text{MoH}_2$  and  $\text{Cp}_2\text{WH}_2$  are stable at these temperatures.<sup>27</sup> There has been some suggestion that changes in metal electronegativity may underlie changes in M–H bond energy.<sup>8a</sup> However, the trend in Mulliken electronegativity of the 4d metals is the reverse of the trend for the 5d metals.<sup>8b</sup> If the  $\text{Cp}_2\text{M}$  group electronegativity is important, it does not follow the trends of the gaseous metal atoms.

The most important determinant of  $\nu(\text{MH}_n)$  is the metal itself; this effect may even be seen to continue outside the  $\text{Cp}_2\text{MH}_n$  series where  $\nu(\text{MH})$  still increases with atomic number.<sup>15,28</sup> These trends contrast with those for  $\nu(\text{CO})$  of metal carbonyls, for which there is often no change on moving from 3d to 4d to 5d elements and a change of only ca. 40  $\text{cm}^{-1}$  on changing atomic number by one unit. However, metal carbonyls exhibit a substantial decrease in  $\nu(\text{CO})$  on increasing the number of CO ligands and an even more marked decrease with increasing positive charge.<sup>29</sup> The trends in the totally symmetric  $\nu(\text{MC})$  of metal carbonyls are less well documented, but they seem considerably closer to our observations on  $\nu(\text{MH}_n)$ .<sup>28</sup> Our understanding of MH vibrations still leaves much to be desired. We hope that these data will provide stimulus for further theoretical studies.<sup>26,30</sup>

**Bandwidth and Splitting of  $\nu(\text{MH}_n)$ .** Almost all the spectra reveal either broad  $\nu(\text{MH}_n)$  bands (solutions) or multiple com-

ponents (matrices). The explanations canvassed in part IV of Results included (a) multiple fundamentals, (b) coincident overtone and combination bands, (c) multiple conformations, and (d) multiple matrix or solution sites. The comparison of matrix IR and Raman spectra of  $\text{Cp}_2\text{WH}_2$  rule out (a); in any case there are too many components. The evidence from partially deuterated complexes does not support explanations involving Fermi resonance with overtones as in (b). If explanation d is to hold, there should be large external solvent effects. The experimental data exclude this too:  $\text{Cp}_2\text{WH}_2$  1905  $\text{cm}^{-1}$  (Ar), 1900  $\text{cm}^{-1}$  (CO), 1908  $\text{cm}^{-1}$  ( $\text{CH}_4$ );  $\text{Cp}_2\text{MoH}_2$  1830  $\text{cm}^{-1}$  (fwhm 43  $\text{cm}^{-1}$ ) ( $\text{C}_6\text{H}_{12}$  solution), 1833  $\text{cm}^{-1}$  (fwhm 42  $\text{cm}^{-1}$ ) (thf solution). One type of conformational effect would involve variations in the geometry of the  $\text{MH}_2$  group in which the HMH bisector moved out of coincidence with the XMX bisector while the  $\text{MH}_2$  group remained in the same plane:



If so we might expect a very low frequency and large amplitude deformation vibration. However, our data suggest that all three IR-active  $\text{MD}_2$  deformation modes lie above 400  $\text{cm}^{-1}$ .

We conclude that it is the conformation of the  $\text{C}_5\text{H}_5$  rings that broadens the MH stretching modes inhomogeneously in solution and splits them in matrices. In most matrices the ring rotation must be frozen out so that we see individual components. It follows that the barrier to ring rotation must arise in large measure from interference between hydrogen atoms or between hydrogen and carbon atoms during vibration. Using the neutron diffraction data on  $\text{Cp}_2\text{MoH}_2$ , we have calculated minimum equilibrium distances from the hydridic hydrogen to ring carbon and hydrogen of  $\text{H}\cdots\text{C} = 2.37$  Å and  $\text{H}\cdots\text{H} = 2.45$  Å.<sup>22</sup> In comparison with the sum of the van der Waals radii of ca. 2.9 Å and the sum of the half-angle radii of 2.17 Å<sup>31</sup> (applicable properly to molecules containing atoms of the first row of the periodic table), this C...H contact is consistent with steric interference with the rings during M–H vibrations. The conformational effects also lead to an explanation of the discrepancy between IR and Raman maxima of  $\text{Cp}_2\text{ReH}$  in solution. The most intense components in each spectrum must represent different conformers.

**Acknowledgment.** We are most grateful to Dr. A. J. Downs and Professor R. E. Hester for the use of their Raman spectrometers and to Dr. J. S. Ogden and A. K. Brisdon for performing force constant calculations. This work was supported by an SERC equipment grant.

**Note Added in Proof.** Since submitting this paper, we have recorded the Raman spectrum of  $\text{Cp}_2\text{TaH}_3$  in thf solution. The data are included in Table II but not in Figure 7. No significant adjustment is required to the parameters in the general equations of the Discussion, although the rms errors are slightly reduced.

**Supplementary Material Available:** Table III, wavenumbers of matrix-isolated  $\text{Cp}_2\text{MH}_n$  and isotopic derivatives below 2100  $\text{cm}^{-1}$  (5 pages). Ordering information is given on any current masthead page.

- (26) Lauher, J. W.; Hoffmann, R. *J. Am. Chem. Soc.* **1976**, *98*, 1729.  
 (27) Tebbe, F. N.; Parshall, G. W. *J. Am. Chem. Soc.* **1971**, *93*, 3793.  
 Barefield, E. K.; Parshall, G. W.; Tebbe, F. N. *J. Am. Chem. Soc.* **1970**, *92*, 5234.  
 (28) Nakamoto, K. "Infrared and Raman Spectra of Inorganic and Coordination Compounds", 3rd ed.; Wiley: New York, 1978.  
 (29) Timney, J. A. *Inorg. Chem.* **1979**, *18*, 2502.  
 (30) Bursten, B. E.; Gatter, M. G. *J. Am. Chem. Soc.* **1984**, *106*, 2554; *Organometallics* **1984**, *3*, 895. Ziegler, T. *Organometallics* **1985**, *4*, 675.

- (31) Bartell, J. S. *J. Chem. Phys.* **1960**, *32*, 827. Glidewell, C. *Inorg. Chim. Acta* **1975**, *12*, 219.